

Experiences with sonic nozzles used for different gases and wide range of pressure and temperature conditions

Bodo Mickan, Rainer Kramer
Physikalisch-Technische Bundesanstalt PTB
Bundesallee 100
D-38116 Braunschweig, Germany
Phone: ++49 (0) 531 592 1331
Fax: ++49 (0) 531 592 69 1331
e-mail: bodo.mickan@ptb.de

Abstract: In the past years sonic nozzles were used in several inter-comparisons as transfer standards (e.g. [1], [2]) and are assumed as the most stable artefacts. Nevertheless, the aim of the flow community to establish inter-comparisons including facilities with different operating ranges, different gases and wide ranges of temperature and pressure conditions needs a careful evaluation of the potential artefacts for such inter-comparisons. In this respect the influences of the operating conditions to the calibration values of sonic nozzles will be discussed in this paper and conclusions will be made.

The base for the discussion in this paper is a set of measurements with sonic nozzles operated in a pressure range between 80 kPa and 5000 kPa, a temperature range of -2°C to 23°C and with gases humid air, dry air, nitrogen and natural gas.

1. Introduction

The background for the investigations explained below was a customer order¹ for calibration of sonic nozzles which shall be used with nitrogen under pressure up to 5000 kPa. As the PTB has no facility to perform such calibration in their laboratory, it was decided to look for opportunities to calibrate the nozzles on site and to support the reliability of this calibration by accompanying measurements at the standard flow facilities of PTB. Hence, we got a quite large set of measurements results to determine the discharge coefficient of six sonic nozzles based on measurements in up to four different set ups, different gases as well as very different pressure and temperature conditions. This is a situation which is comparable to the situation of an inter comparison with participants using different fluids under different operating conditions. Therefore the evaluation of the experiments described below and the conclusions out of it will be an useful input to the ongoing discussion in the flow community about the systematic impacts of fluid properties and test conditions to the results of inter comparisons.

2. The experimental set up

2.1 The critical nozzles under test

The six critical nozzles under test were specified as toroidal nozzles according to the ISO9300 [3] with throat diameters between about 1 mm to 11.25 mm (see also table 1). The divergent angle of the diffuser was specified with 4°.

After manufacturing the inner dimensions of the nozzles were measured by an accredited laboratory for length measurements (DKD). The result of these measurements demonstrates the real life concerning the manufacturing of sonic nozzles. In Fig. 1 the curvature ratio Ω (i.e. the inverse of the curvature radius normalized by the throat diameter) is shown for each nozzle as well as the requirement of the ISO standard for this value. It is more than obviously that these nozzles do not fit to the requirement of the ISO standard. Especially near to the throat the deviations are remarkable high and very different for each nozzle. Only the three larger nozzles have a curvature near to the specified value of 0.5 upstream to the throat (i.e.

¹ We acknowledge to BASF Aktiengesellschaft, 67056 Ludwigshafen am Rhein, for their kind cooperation and support for all these investigations.

at negative values for normalized position z/d) but even here not fitting to the tolerance band of the ISO standard.

Despite of this fact it was decided to proceed with these nozzles because it was not the intention to make use of the ISO standard for the calibration value. But finally it is also interesting to look to the results for discharge coefficient of these nozzles in comparison with the standard values. This will be shown below in chapter 3.4.

2.2 PTB Air Flow Standards

In the following we give a very short description of the test arrangements and their traceability. Some more information about test conditions especially pressures and temperatures is given in table 1.

The first flow standard used here was the PTB bell prover [4] which is used to calibrate sonic nozzles at flows less than $< 100 \text{ m}^3/\text{h}$ with humid atmospheric air at an uncertainty level of 0.06 % ($k=2$) for the flow rate². This calibration capability of PTB has the CMC entry number DE41 at the BIPM data base. The nozzles are operated downstream to the bell prover as shown in Fig 2 I.

Customer meters or transfer meters with flow rates larger than $100 \text{ m}^3/\text{h}$ are calibrated in PTB using a sonic nozzles rig [5] (see Fig. 2 II, CMC entry DE43) which traceability chain starts with the PTB bell prover. The uncertainty for flow rate is about 0.08 % ($k=2$).

The calibration of sonic nozzles needs a further step, because the capacity of the vacuum pumps does not allow a calibration of two nozzles in series. Therefore we calibrate first a transfer meter with good reproducibility and then we calibrate the nozzle with the transfer meter. The pressure losses inside the test rigs allow us to vary the inlet pressure of the nozzles under test over a range of about 90 kPa to 100 kPa. From principle the set up is identical to Fig 2 II (nozzle downstream to the transfer meter). Finally, we claim an uncertainty of $U = 0.12 \%$ ($k=2$) for the flow rate value of a nozzle of such a size calibrated with air at atmospheric conditions.

The third arrangement (shown in Fig. 2 III) is using (dry) pressurized air. This calibration set up of PTB is relatively new and was used in this way successfully in the CCM.FF-K6 [1] in the year 2005. The principle is to operate the meters (nozzles) under test with the operating pressure up to 700 kPa, decompress downstream the air back to ambient pressure and apply at this pressure level a transfer meter calibrated at the sonic nozzle test bench (DE43, as described above). The central challenge is to keep the temperature conditions for the transfer meter close to the conditions of its calibration to avoid systematic impacts here. Therefore a temperature conditioning can be applied upstream to the set-up. With temperatures close to ambient conditions (as laid down in table 1 for these measurements) we claim an expanded uncertainty $U = 0.15 \%$ ($k = 2$) for the flow rate. The transfer meter used here was a pulsation free rotary meter with pipe size 50 mm (see also table 2, meter #1).

The composition of the air used at PTB is always the standard composition of dry air with compensation for humidity (measured with dew point meters). The influence of the humidity is calculated as given in Aschenbrenner [6]. Density and compressibility are calculated in accordance to Giacomo [7].

² The error bars in the Fig. 4 to 9 for the discharge coefficients indicate the uncertainties of the flow rate measurements only. We refrain here from explicit considering of further contributions (like throat diameter or critical flow factor) because we use them only to illustrate the relative deviations among the measurements and made no further detailed use in evaluations.

2.3 PTB / *pigsar* Flow Standard for natural gas

The two largest nozzles fall with their nominal flow rate into the operating range of the *pigsar* test facility. Hence, we made use of calibrations at *pigsar* to get further information about the nozzles at high pressure conditions.

The *pigsar* test facility uses natural gas at pressures between 16 and 50 bar. It is described in detail in the references [8] [9]. The traceability is based on the geometrically measured volume of a high pressure piston prover and gas density measurements made with a buoyancy balance.

The natural gas used at *pigsar* is a North Sea gas from the Groningen region. The critical flow factor, C^* is calculated using the AGA8-DC92 state equations according to Schley [10].

The uncertainty for calibration value of a sonic nozzle at *pigsar* can be claimed with 0.15 %.

2.4 Test rig with nitrogen

The central intention of the customer (BASF) was the establishing of defined constant mass flow rates of nitrogen for their purposes in chemical experiments. The principle outline of arrangement to reach this is shown in Fig. 2 IV.

The nitrogen is supplied from high pressure network (operating at about 300 bar). After the decompression down to a level of 50 bar it supplies the test rig. At the entrance of the test rig a pressure control valve is used to set the pressure to the actual needed values. The central idea of the rig is to control the pressure at the level which one needs to get a nearly constant mass flow rate through the nozzle considering the actual measured temperature at the nozzle entrance. The temperature at the nozzle entrance is changing and sometimes far away from normal ambient conditions due to the high decompression of the nitrogen and the absents of any temperature conditioning upstream to the nozzle. To be able to operate the PTB transfer meters at reasonable and stable conditions the application of a controlled heater was necessary.

Fig. 3 shows typical values for the relevant pressures and temperatures at nozzle and transfer meter as well as the calculated mass flow rate and the experimental determined discharge coefficient versus time.

For this calibration on site we applied again rotary meter and turbine as transfer meters which were calibrated at PTB flow standards as described above. We used three different meters (see table 2, meters #2 to #4) with a quite good overlapping in the flow rate range. This gave the opportunity to test at several points with these three meters under identical conditions and to detect therefore systematic impacts due to potential installation effects.

It is a specialty of the equipment at the BASF test rig to use temperature sensors with a low inertia against temperature changes. Secondly they are mounted without a temperature tap with direct contact to the gas flow and are therefore less influenced by differences between ambient temperature and gas temperature. We see this as an important factor to reach the characteristic of the test rig and its control loops.

3. The experimental results and their evaluation

All measurement results in form of the discharge coefficient c_D of the sonic nozzles are shown in the Fig. 4 to Fig. 9. These discharge coefficients are plotted versus the inverse square root of the Reynolds number. This emphasizes the range of operation with laminar boundary layers inside of the nozzles which typically occurs for Reynolds numbers $Re < 10^6$ ($1/Re^{0.5} > 0.001$).

One of the central aims was the comparison of calibration quality among the different test arrangements and test conditions. The measurement campaigns do normally not overlap in

the Reynolds range, hence we needed some common reference line over the complete range to evaluate the potential differences between the results out of different campaigns. For this purpose we made use of a mathematical modeling covering not only the laminar but also the turbulent regime and the transition between both.

3.1 Mathematical modeling of the discharge coefficient

When a sonic nozzle is operated definitely either in laminar or turbulent regime, the dependency of the discharge coefficient on the Reynolds number can be described by following two equations where we have the three parameters a , b_{lam} and b_{turb} to characterize the behavior of a specific nozzle (for a detailed explanation please refer e.g. also [11]):

$$c_{D,lam} = a - b_{lam} \cdot Re^{-0.5} \quad (1)$$

$$c_{D,turb} = a - b_{turb} \cdot Re^{-0.139} \quad (2)$$

In the so called transition region between the range of laminar and turbulent boundary layers we find values in between the two curves (1) and (2) connecting them with an smooth curve. To simulate this behavior we make use of two so called “switching” functions s_{off} and s_{on} :

$$s_{off} = 0.5 \left\{ 1 - \tanh \left[k_{tr} \log \left(\frac{Re}{Re_{tr}} \right) \right] \right\} \quad (3)$$

$$s_{on} = 0.5 \left\{ 1 + \tanh \left[k_{tr} \log \left(\frac{Re}{Re_{tr}} \right) \right] \right\} \quad (4)$$

With the parameter Re_{tr} one can adjust the location and with k_{tr} the “speed” (range) of the transition. The sum of s_{off} and s_{on} is always unity.

With this we can define a complete function for the discharge coefficient c_D with only five parameters to cover the laminar as well as the turbulent region including the transition:

$$c_D = s_{off} \cdot c_{D,lam} + s_{on} \cdot c_{D,turb} \quad (5)$$

For the determination of the parameters in eq. (1) to (4) we applied different strategies: least square fits, theoretical based calculations [11] and arbitrary set values to cover some general experiences.

The theoretical based calculations [11] can deliver only values for the parameters a , b_{lam} and b_{turb} . For the “transition parameters” Re_{tr} and k_{tr} we have to set here arbitrary values of $Re_{tr} = 1.3 \cdot 10^6$ and $k_{tr} = 12$ which are in good agreement with former results e.g. published in [2]. Furthermore, the value $k_{tr} = 12$ sets the begin and end of transition to a ratio of $Re_{end\ transition} / Re_{begin\ transition} \approx 2$ which agrees with general statements about laminar-turbulent transitions (see e.g. [12] for an overview to this).

The tools for nonlinear least square fits can determine of course all five parameters if sufficient enough data are available. The data base here is different for the several nozzles in this aspect. Therefore in each case it was decided either to refrain to calculate some of the parameters or to set them also as arbitrary fixed values.

Table 3 gives the overview of all the parameter values. Values in brackets indicate arbitrary fix values as described here.

3.2 Measurements at PTB with atmospheric air and dry pressurized air

The results measurements with atmospheric air and dry pressurized air are all located in the region of laminar boundary layers ($Re^{-0.5} > 0.001$). Therefore we obtain here an impressive

linear dependency on $Re^{-0.5}$ in the plots Fig. 4 to Fig. 9 as also predicted by eq. (1). The deviations of the measurements results to the curve determined by the least square fit are impressive small (not exceeding 0.05 %) what is a strong indication of the quality of tests using transfer meters downstream to sonic nozzles.

The comparison of the theoretical calculated curves with the fitted curves shows some small deviations. At one hand they can be shifted because of the systematic impact of the value for throat diameter using it for calculation of the discharge coefficients. On the other hand the calculation tool is also limited in its possibilities to predict the correct slope but the difference of slope is fortunately rather constant versus the Reynolds range. Therefore we can make use also of the theoretical predicted curves for an visual evaluation of the measurement results.

3.3 Measurements at BASF with nitrogen and at *pigsar* with natural gas

Only the measurements with nitrogen and natural gas for the nozzles #4 to #6 reached significantly the region of transition between laminar and turbulent boundary layers as well as the turbulent region. Outgoing from the very positive conclusion for the measurements with transfer meters downstream to sonic nozzles at the PTB air flow standards, we can conclude the same here also for the measurements with nitrogen.

Additionally we like to emphasize here:

- Even we made use of three different transfer meters for nitrogen we found a reasonable scatter of these results compared to the claimed uncertainty for flow rate measurement.
- We have an impressive connection using nozzle #5 for measurements air/nitrogen as well as nitrogen/natural gas (Fig. 8).
- For nozzle #5 and #6 the temperature conditions were very far away from the conditions in calibrations with air and natural gas. Nevertheless the consistency of all these results is much better than one can expect from the measurement uncertainties and there is systematic impact to be detecting (we assume 0.05 % as a detection limit in these experiments)
- The results with nozzle #5 and #6 in connection with the very positive conclusion for measurements with pressurized air and nitrogen demonstrate again the consistency between the two independent traceability for air flow at low pressure and natural gas at high pressure conditions at PTB.

3.4 Comparison with ISO9300

Last but not least we like to compare our results for discharge coefficients determined out of the measurements with the values defined in the ISO9300. Outgoing from the large deviations of the real shape of the nozzles from the requirements of the standard one would not expect any reasonable agreement.

In Fig. 10 we summarized all single values for the discharge coefficient of all nozzles. In this plot a statement about the uncertainty of throat diameter is important, but we refrain here from given any definite value. The claimed uncertainty of the laboratory for dimensions is about 1 μ m for a single length but we have to assume higher uncertainty for the characterization of the nozzles out of a grid of coordinates points.

Nevertheless, we can find in Fig. 10 an astonishing agreement of all results not only with the ISO value for normal machined nozzles (curve ISO9300(1) in Fig. 10) but also for the so called high precision nozzles curve ISO9300(2) in Fig. 10).

4. Conclusions

The calibration of six sonic nozzles under quite different test conditions and in different arrangement was a unique opportunity to investigate potential systematic impacts to the calibration values of the nozzles depending on fluids, temperature or pressures. Hence, we assume this experimental work as good base for preparation of new inter comparisons for gas as they are under discussion in the fluid flow community.

The test arrangements covers at one hand calibration capabilities which are already proofed within international key comparisons (CCM.FF-K5a [13] and CCM.FF-K6 [1], but also [2]) and on the other hand calibrations on customer site performed by PTB with transfer meters. As the proofed calibration capabilities of PTB covers the lower end as well as the upper end of the calibration range of these nozzles investigated here, we got a reliable proof of the calibrations on site of the customer.

The uncertainties of the flow rate measurements ranges from 0.06% to 0.15%. The differences obtain between the different test arrangements are in the order of less than 0.05 %. Therefore the measurements showed an high consistency independent to:

- the traceability (PTB bell prover or PTB high pressure piston prover)
- the test fluid (air, nitrogen, natural gas)
- the test arrangement
- the transfer meter used for measurements
- temperature and pressure conditions at entrance of the sonic nozzles.

Furthermore it could be demonstrated that the discharge coefficient of sonic nozzles can be described mathematically by a reasonable simple model with only five parameters.

5. Tables and figures

Table 1: List of test conditions and arrangements. For arrangements see also Fig. 2

Nozzle	d_{Throat} [mm]	test conditions at nozzle entrance	arrangements
#1	0,9915	humid air: $p = 80.5 \dots 101$ kPa $\vartheta = 21.9 \dots 22.2$ °C $h = 40 \dots 45$ %	test arrangement Fig.2 I
		dry air: $p = 161.4 \dots 601.3$ kPa $\vartheta = 22.3 \dots 22.5$ °C $h = 7 \dots 9$ %	test arrangement Fig.2 III transfer meter #1
#2	1,3436	humid air: $p = 80.5 \dots 102.2$ kPa $\vartheta = 21.7 \dots 22.0$ °C $h = 40 \dots 45$ %	test arrangement Fig.2 I
		dry air: $p = 160.7 \dots 597.9$ kPa $\vartheta = 22.3 \dots 22.5$ °C $h = 7 \dots 9$ %	test arrangement Fig.2 III transfer meter #1
		nitrogen $p = 1687 \dots 4872$ kPa $\vartheta = 14.9 \dots 17.5$ °C	test arrangement Fig.2 IV transfer meter #2
#3	2,295	humid air: $p = 79.83 \dots 100.9$ kPa $\vartheta = 22.7 \dots 22.9$ °C $h = 45 \dots 50$ %	test arrangement Fig.2 I
		dry air: $p = 160.7 \dots 587.5$ kPa $\vartheta = 21.7 \dots 21.9$ °C $h = 7 \dots 9$ %	test arrangement Fig.2 III
		nitrogen $p = 1687 \dots 4944$ kPa $\vartheta = 14.9 \dots 19.0$ °C	test arrangement Fig.2 IV transfer meters #2 + #3
#4	3,903	humid air: $p = 80.6 \dots 100.8$ kPa $\vartheta = 22.7 \dots 22.9$ °C $h = 45 \dots 50$ %	test arrangement Fig.2 I
		dry air: $p = 157.5 \dots 600.8$ kPa $\vartheta = 20.6 \dots 20.8$ °C $h = 7 \dots 9$ %	test arrangement Fig.2 III transfer meter #1
		nitrogen $p = 1680 \dots 4958$ kPa $\vartheta = 8.2 \dots 16.0$ °C	test arrangement Fig.2 IV transfer meters #2, #3 + #4
#5	6,646	humid air: $p = 91.4 \dots 102.6$ kPa $\vartheta = 22.0 \dots 22.2$ °C $h = 35 \dots 40$ %	test arrangement Fig.2 II transfer meter #1
		dry air: $p = 132.0 \dots 602.9$ kPa $\vartheta = 19.2 \dots 21.8$ °C $h = 7 \dots 9$ %	test arrangement Fig.2 III transfer meter #1
		nitrogen $p = 552 \dots 2392$ kPa $\vartheta = -1.3 \dots 9.6$ °C	test arrangement Fig.2 IV transfer meters #2, #3 + #4
		natural gas $p = 2144 \dots 5001$ kPa $\vartheta = 17.4 \dots 20.3$ °C	tested at <i>pigsar</i>
#6	11,261	humid air: $p = 85.0 \dots 101.3$ kPa $\vartheta = 20.5 \dots 20.8$ °C $h = 30 \dots 35$ %	test arrangement Fig.2 II transfer meter #1
		nitrogen $p = 358 \dots 841$ kPa $\vartheta = -1.9 \dots 8.4$ °C	test arrangement Fig.2 IV transfer meters #2, #3 + #4
		natural gas $p = 2150 \dots 5082$ kPa $\vartheta = 16.5 \dots 19.2$ °C	tested at <i>pigsar</i>

Table 2: List of transfer meters used for nozzle calibration

Transfer meter	type	Pipe size	Flow range
#1	pulsation free rotary meter (Actaris S-Flow)	50 mm	0.5 to 190 m ³ /h
#2	dual rotary meter	100 mm	2 to 320 m ³ /h
#3	turbine meter	150 mm	80 to 1600 m ³ /h
#4	turbine meter	200 mm	250 to 2500 m ³ /h

Table 3: List of parameters in eq. (1) to (4) determined by LSF and based on geometry acc. [11].

Nozzle	parameter	Fitted from experiment	Based on geometry [11]	remarks
#1	a	0.99607	0.99743	Operation in laminar range only ($Re \leq 1e6$)
	b_{lam}	2.98107	3.10391	
	b_{turb}	--	--	
	k_{tr}	--	--	
	Re_{tr}	--	--	
#2	a	0.99510	0.99611	Operation in laminar range only ($Re \leq 1e6$)
	b_{lam}	2.73673	2.91178	
	b_{turb}	--	--	
	k_{tr}	--	--	
	Re_{tr}	--	--	
#3	a	0.99375	0.99663	Operation in laminar range only ($Re \leq 1e6$)
	b_{lam}	2.69883	2.97732	
	b_{turb}	--	--	
	k_{tr}	--	--	
	Re_{tr}	--	--	
#4	a	0.99493	0.99581	The values for k_{tr} and Re_{tr} are set both according to the experience in [2]
	b_{lam}	2.44536	2.87805	
	b_{turb}	0.03251	0.025991	
	k_{tr}	(12)	(12)	
	Re_{tr}	(1.3e6)	(1.3e6)	
#5	a	0.99907	0.99935	The value for k_{tr} is set according to the experience in [2]; Re_{tr} out of fit also used for calc.
	b_{lam}	3.3509	3.77728	
	b_{turb}	0.05616	0.034186	
	k_{tr}	(12)	(12)	
	Re_{tr}	1284246	(1.284e6)	
#6	a	0.99805	0.99981	The value for k_{tr} is set according to the experience in [2]; Re_{tr} out of fit also used for calc.
	b_{lam}	4.04794	4.46807	
	b_{turb}	0.04118	0.03853	
	k_{tr}	(12)	(12)	
	Re_{tr}	1393908	(1.394e6)	

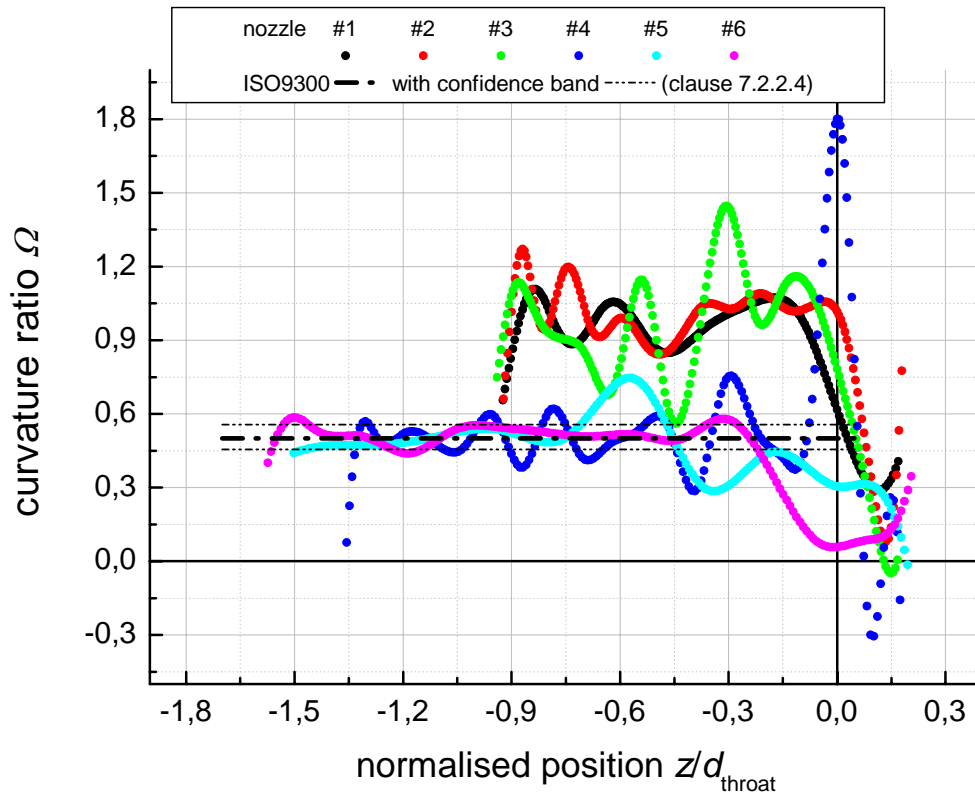


Fig. 1: The curvature ratios Ω of the nozzles under test in comparison with the requirement of the ISO9300.

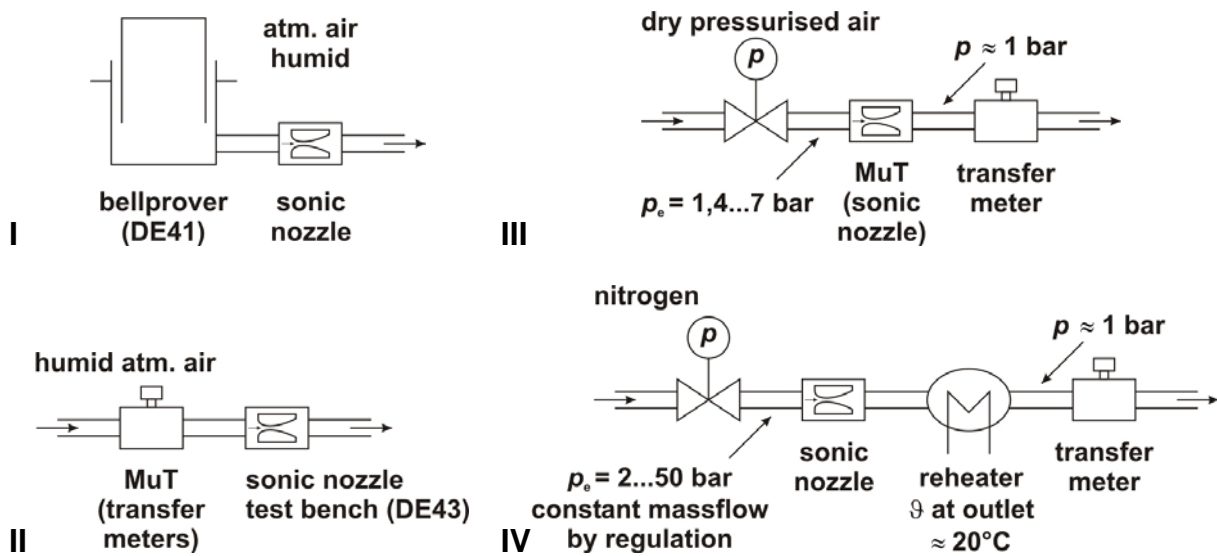


Fig. 2: The several test arrangements for air (I to III) and nitrogen (IV) used for the investigations.

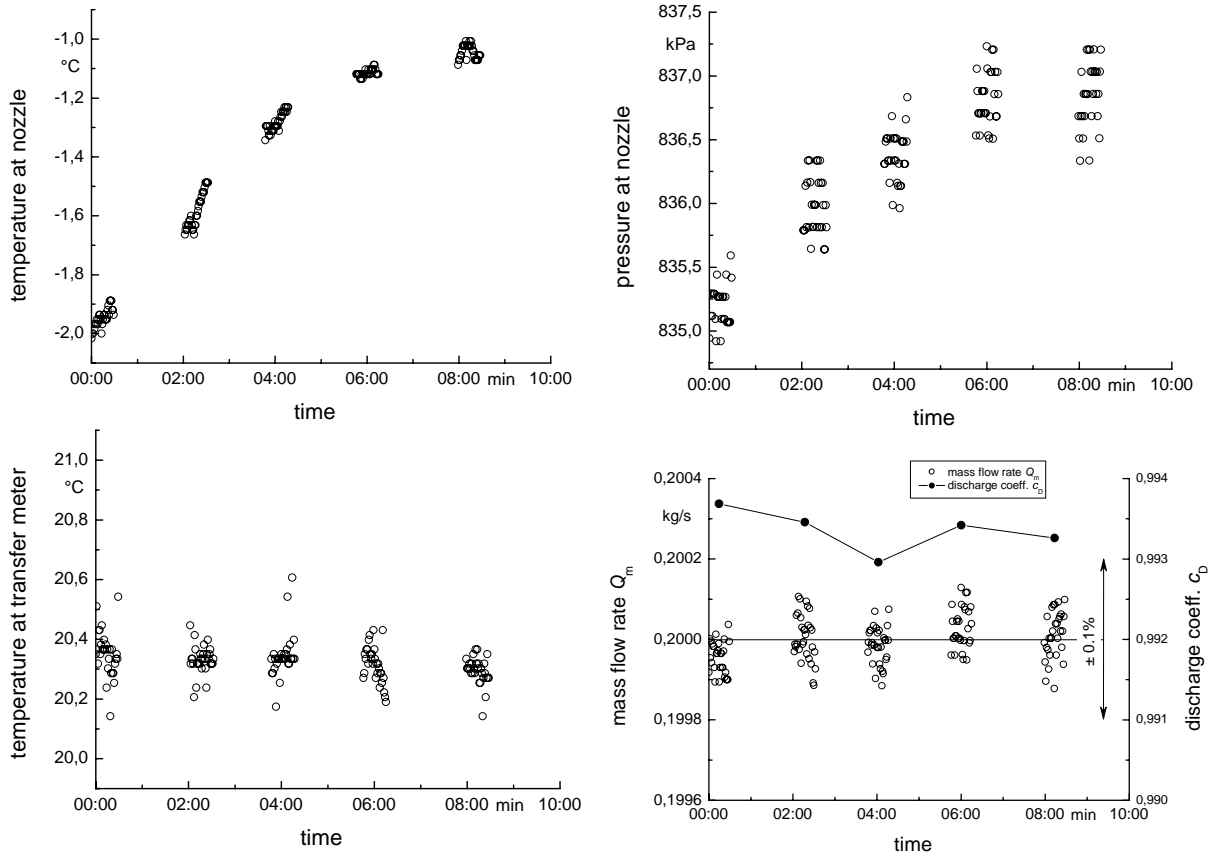


Fig. 3: Typical examples for temperatures and pressures at the nozzle, temperature at transfer meter, mass flow rate (calculated from entrance conditions of the nozzle) and determined discharge coefficient versus time.

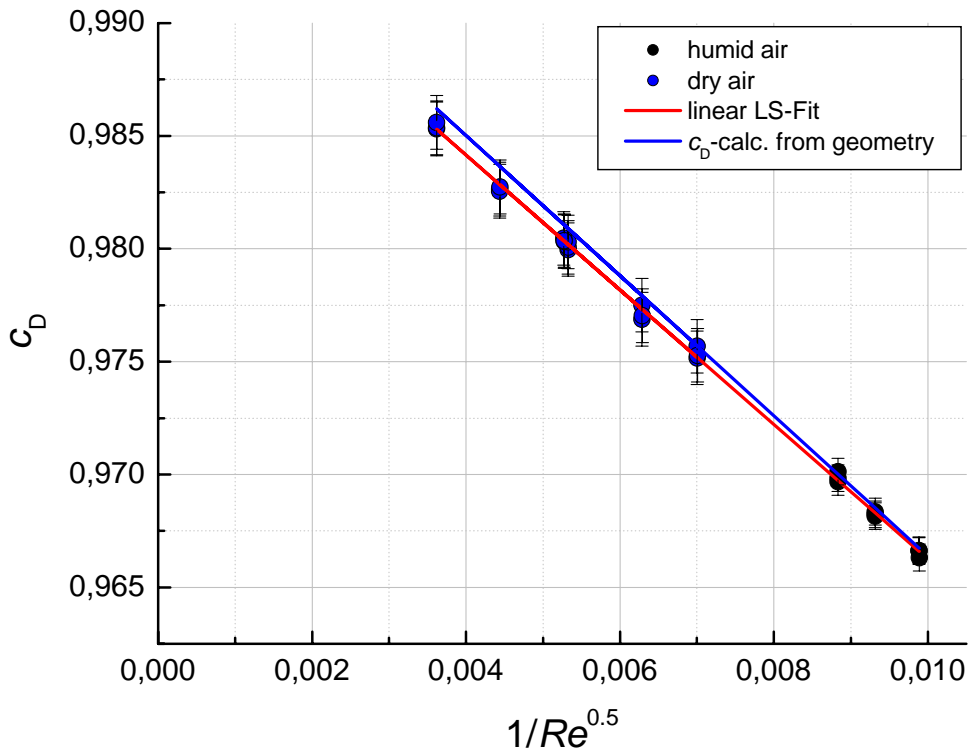


Fig. 4: Discharge coefficient c_D for nozzle #1 from experiments as well as calculated based on geometry [11]. For test conditions and arrangements see table 1.

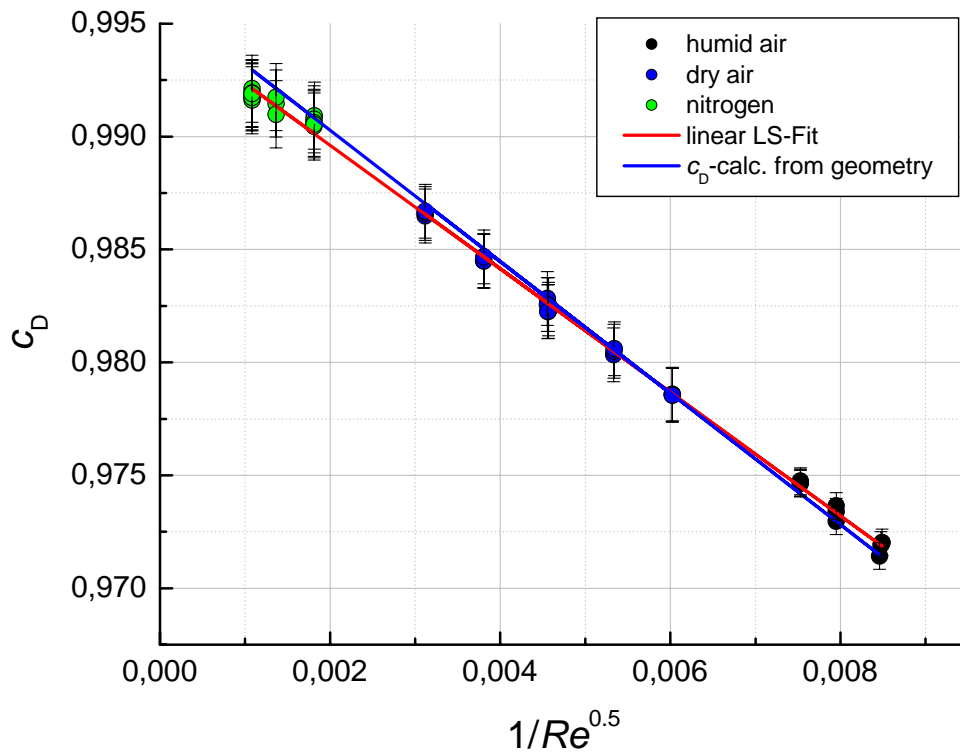


Fig. 5: Discharge coefficient c_D for nozzle #2 from experiments as well as calculated based on geometry [11]. For test conditions and arrangements see table 1.

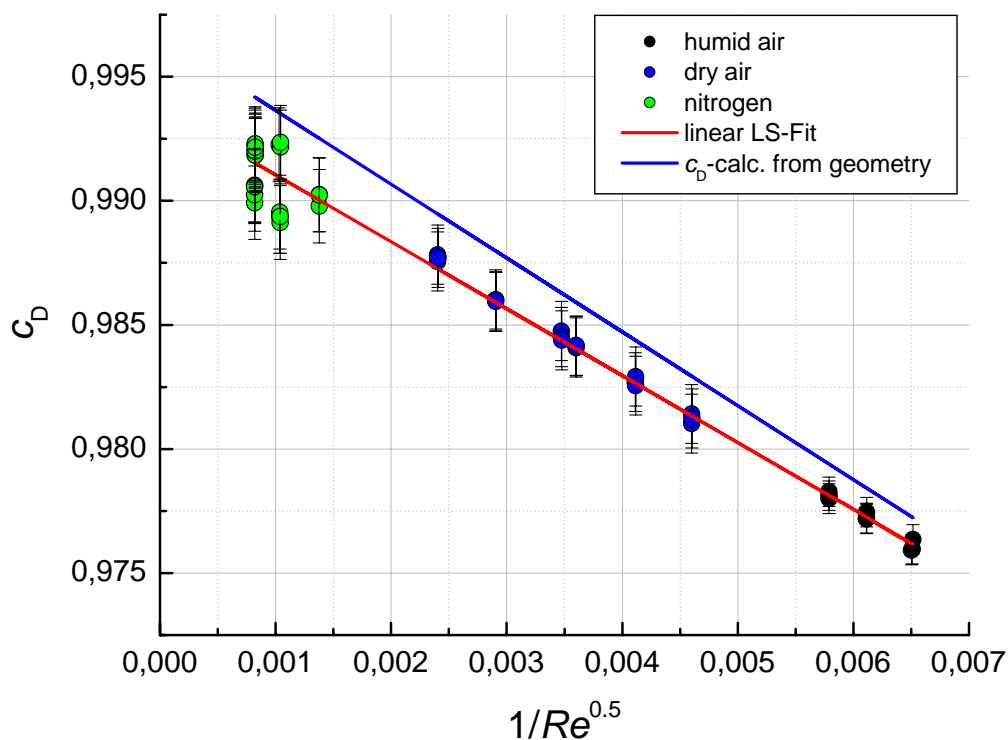


Fig. 6: Discharge coefficient c_D for nozzle #3 from experiments as well as calculated based on geometry [11]. For test conditions and arrangements see table 1.

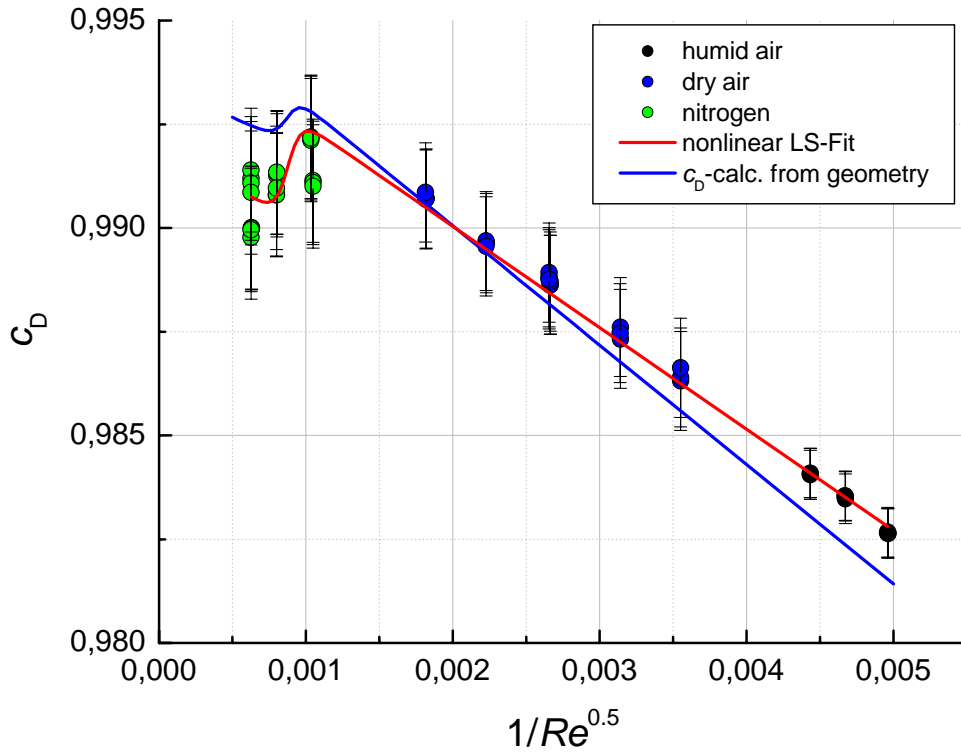


Fig. 7: Discharge coefficient c_D for nozzle #4 from experiments as well as calculated based on geometry [11]. For test conditions and arrangements see table 1.

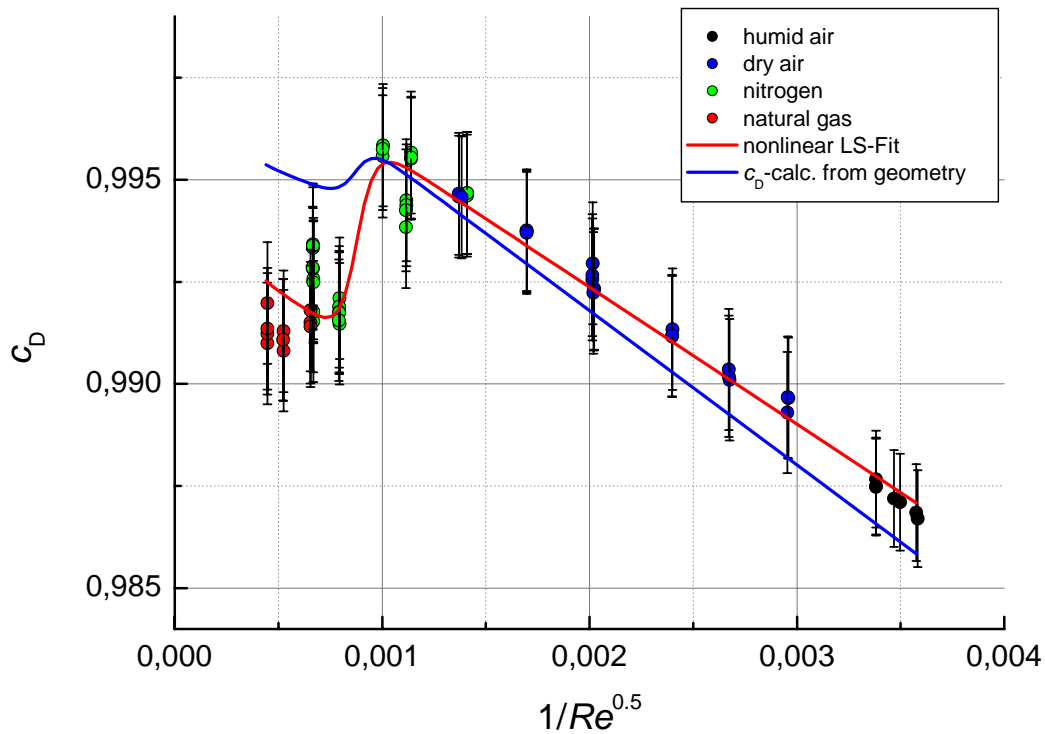


Fig. 8: Discharge coefficient c_D for nozzle #5 from experiments as well as calculated based on geometry [11]. For test conditions and arrangements see table 1.

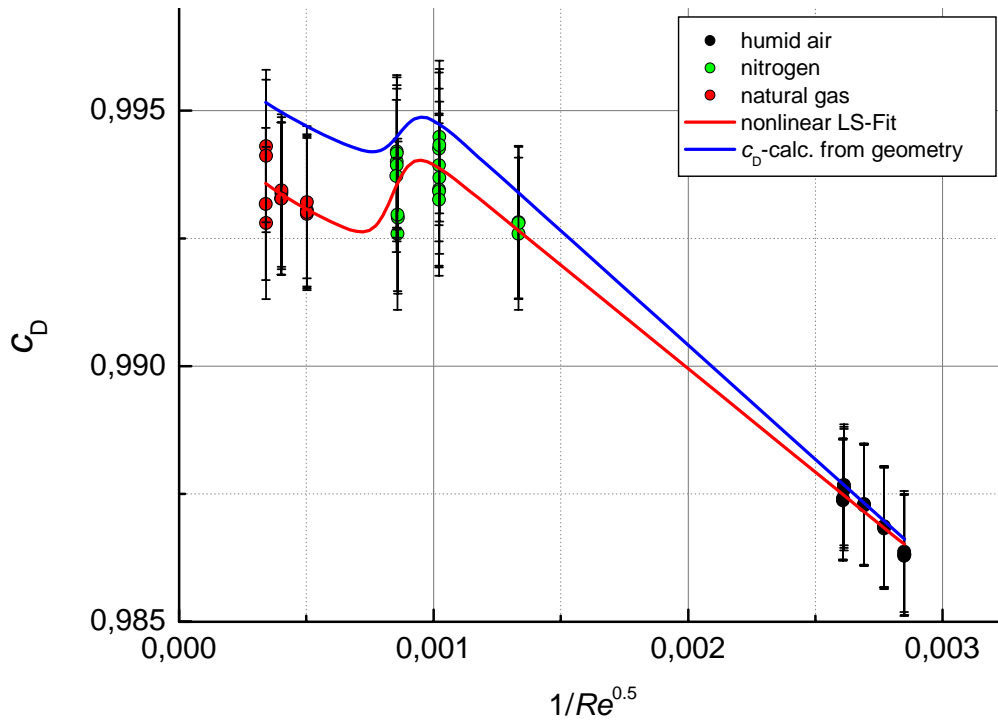


Fig. 9: Discharge coefficient c_D for nozzle #6 from experiments as well as calculated based on geometry [11]. For test conditions and arrangements see table 1.

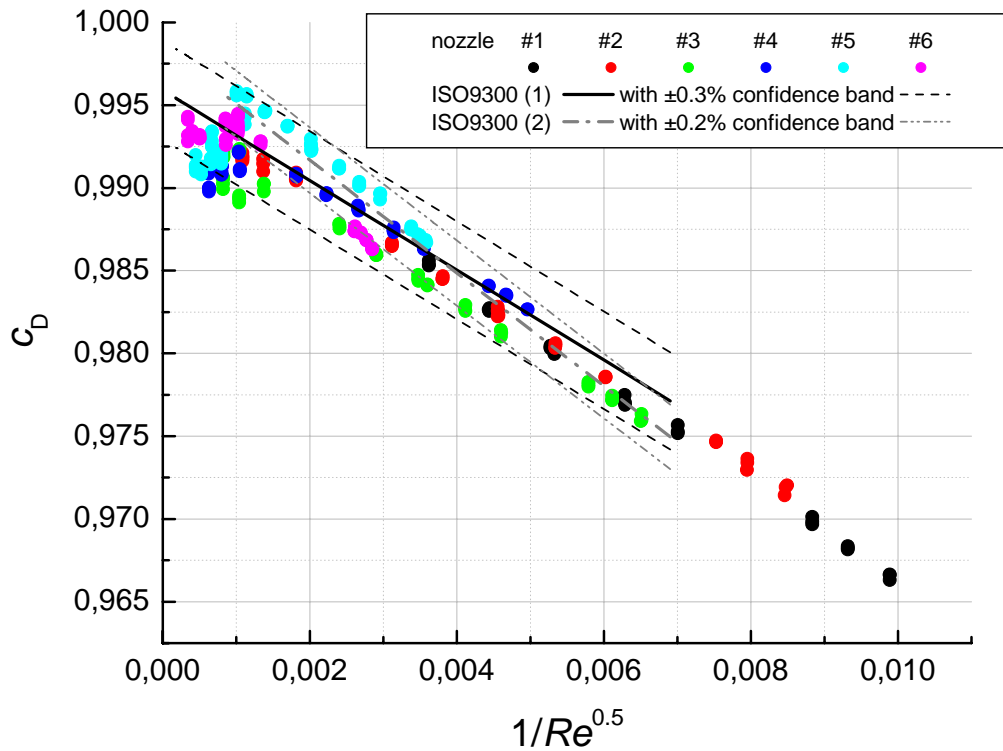


Fig. 10: Overview off all discharge coefficients c_D for nozzles #1 to #6 from experiments in comparison to definitions in ISO9300 [3].

6. References

- [1] *CIPM Key Comparison for Low-Pressure Gas Flow: CCM.FF-K6, Final Report*; John Wright, Bodo Mikan, Richard Paton, Kyung-Am Park, Shin-ichi Nakao, Khaled Chahine, Roberto Arias; October 9, 2007;
http://kcdb.bipm.org/AppendixB/appbresults/ccm.ff-k6/ccm.ff-k6_final_report.pdf
- [2] Mickan, B., Kramer, R., Dopheide, D., Hotze, H.-J., Hinze, H.-M., Johnson, A., J. Wright, J., Vallet, J.-P., *Comparisons by PTB, NIST, and LNE-LADG in Air and Natural Gas by Means of Critical Venturi Nozzles Agree within 0.05 %*, Proceedings of the 6th International Symposium on Fluid Flow Measurement, Queretaro, Mexico, May, 2006.
- [3] *International Standards Organization, Measurement of Gas Flow by Means of Critical Flow Venturi Nozzles*, ISO 9300:2005(E).
- [4] Brunnemann, H., Aschenbrenner, A., *Volumen mit Garantie*, mpa 1994, M.9, S. 8-15.
- [5] Aschenbrenner, A., *Calibration of the New Test Rig for Large Gas Meters of the Physikalisch-Technische Bundesanstalt*, VDI-Berichte NR. 768, 1989, ISSN 0083-5560, pp. 11-22.
- [6] Aschenbrenner, A., *The Influence of Humidity on the Flowrate of Air through Critical Flow Nozzles*, *Flow Measurement*, Proceedings of Flomeko 1983, Budapest, North-Holland Publishing Company Amsterdam-New York-Oxford, pp. 71-74.
- [7] Giacomo, P., *Formel für die Bestimmung der Dichte von feuchter Luft*, In: PTB-Mitteilungen 89, 4/79, S. 271 ff.
- [8] Bremser, W., Hässelbarth, W., Hirlehei, U., Hotze, H.-J., Mickan, B., Kramer, R., Dopheide, D., *Uncertainty Analysis and Long-Term Stability Investigation of the German Primary High Pressure Natural Gas Test Facility pgsar*, 11th International Conference on Flow Measurement, FLOMEKO' 2003, Groningen, The Netherlands, 12-14 May 2003, CD-ROM, Session 3, p.21.
- [9] Kramer, R., Mickan, B., Hotze, H.-J., Dopheide, D., *The German High-Pressure Piston Prover at pgsar - the German fundamental standard for natural gas at high pressure conditions*, TechTour to the German High-Pressure National Standard pgsarTM, Ruhrgas AG, Dorsten, 15.-16. May 2003, CD-ROM, S. 1-21.
- [10] Schley, P., *Thermodynamische Stoffgrößen von Erdgasen zur Beschreibung einer kritischen Düsenströmung*, Fortschr.-Ber. VDI Reihe 7 Nr. 418. Düsseldorf: VDI Verlag 2001.
- [11] Mickan, B., Kramer, R., Dopheide, D., *Determination of Discharge Coefficient of Critical Nozzles Based on Their Geometry and the Theory of Laminar and Turbulent Boundary Layers*, Proceedings of the 6th International Symposium on Fluid Flow Measurement, Queretaro, Mexico, May, 2006.
- [12] Hu, K., *Berechnung reibungsbehafteter, kompressibler Düsenströmungen in der Stömungs- und Verfahrenstechnik*, Aachen 1998, ISBN 3-8265-3403-4
- [13] Dopheide D., Mickan B., Kramer R., Hotze H.-J., van der Beek M., Blom G., Vallet J.-P., Gorieu O.: *Final report on the CIPM Key Comparisons for Natural Gas at High-Pressure*, BIPM, Paris, 2004
http://kcdb.bipm.org/AppendixB/appbresults/ccm.ff-k5.a/ccm.ff-k5.a_final_report.pdf